ISSN No:-2456-2165

# Crystallinity, Amorphousity and Characterization of Synthesized $Sb_2O_3$, BaO and NiO Nanoparticles and Nanocomposites

Sabo Yasser Takko, Boryo Doris Ezekiel Amin, Chindo Istifanus Y. Ibrahim Jamila Shekarau
Department of Chemistry, Abubakar Tafawa Balewa University, Bauchi, Nigeria
Corresponding author: Yasser Sabo Takko,

**Abstract:- Nanoparticles were prepared via chemical precipitation method and the nanocomposites were fabricated using in situ method of polymerization. Both nanoparticles and formulated nanocomposites were characterized using X-Ray Diffraction technique (XRD). From the XRD results, it was observed that the crystallite sizesof the synthesized nanoparticles were calculated using a Debye Scherrer's equation and were found to be 31.2 nm for NiO nanoparticles, 46.4 nm for BaO nanoparticlesand 32.3 nm for $Sb_2O_3$ nanoparticles respectively. These results showed that the sizes of the oxide nanoparticles prepared were within the nanoscale region. Also results from X-ray diffraction of nanocomposites confirmed the presence of nano metal oxides in the polystyrene. Conclusively, it was observed that at high concentration of nanoparticles incorporated in the polystyrene, nanocomposite containing 0.5 g of NiO nanoparticles is more crystalline followed by nanocomposite containing 0.7 g of BaO and nanocomposite containing 1 g of $Sb_2O_3$nanoparticles due to more periodicity and preferred crystal orientation. Based on the crystalline nature of the synthesized nanoparticles, it is recommended that during the production of polymer nanocomposites, PS/$Sb_2O_3$, PS/BaO and PS/NiO nanocomposites can be used in electrically conductive devices, as reinforcements in construction of buildings, to hinder or slow down the propagation of fire as well as suitable materials for heat transfer applications.**

***Keywords:-*** *Polystyrene, nanoparticles, nanocomposites, crystallinity.*

## I. INTRODUCTION

The term "nanoparticle" is not usually applied to individual molecules; it usually refers to inorganic materials. Nanoparticles are particles between 1 and 100 nanometres (nm) in size with a surrounding interfacial layer. The interfacial layer is an integral part of nanoscale matter, fundamentally affecting all of its properties. The interfacial layer typically consists of ions, inorganic and organic molecules. Organic molecules coating inorganic nanoparticles are known as stabilizing, capping and surface ligands, or passivating agents (Batista, 2015).Nanoparticles are of great scientific interest as they are, in effect, a bridge between bulk materials and atomic or molecular structures (Heinzerling and Oetken 2018). A bulk material should have constant physical properties regardless of its size, but at the nano-scale size-dependent properties are often observed. Thus, the properties of materials change as their size approaches the nanoscale and as the percentage of the surface in relation to the percentage of the volume of a material becomes significant (Heinzerling and Oetken 2018). For bulk materials larger than one micrometer (or micron), the percentage of the surface is insignificant in relation to the volume in the bulk of the material. The interesting and sometimes unexpected properties of nanoparticles are therefore largely due to the large surface area of the material, which dominates the contributions made by the small bulk of the material (Heinzerling and Oetken 2018). Antimony oxide ($Sb_2O_3$) has wide applications as effective catalyst, retardant, conductive material, functional filler and optical material. In addition, $Sb_2O_3$can also be used as conductive materials, high-efficiency flame retardant synergist in plastics, paints, adhesives and textile back coating (Yuehua *et al.,* 2007 and Cheng *et al.,* 2008). It has been reported that NiO, FeO and CoO nanoparticles were synthesized via co-precipitation method from their respective nitrate solutions (Ashik *et al.,* 2018).

The synthesis of metal and metal oxide nanoparticles has attracted a considerable attention in physical, chemical, biological, medical, mechanical and engineering sciences. Metals and metal oxide nanoparticles have high surface area and high fraction of atoms which is responsible for their fascinating properties which depend on size, shape, composition, morphology and crystalline phase (Prabhavathi *et al.,* 2014). Metal oxides nanoparticles have wide applications in air and water purification, due to their potential oxidation strength, high photo stability and non-toxicity. Some of the commonly used synthetic methods are non-sputtering, solvo-thermal, sol-gel, reduction and electrochemical technique, but these methods are costly and involve high pressure and high energy requirement (Prabhavathi *et al.,* 2014).According to Biron (2007), polystyrene is an amorphous thermoplastic polymer that softens at relatively low temperatures and it flows like a liquid at 100 $^oC$ or under stress, making it easy to thermoform or extrude. Service temperatures can be lowered under stress because of modulus decay, creep, strain, relaxation, etc (Biron, 2007). The presence of phenyl groups is responsible for the relatively high glass transition temperature (*T*g) and high refractive index value (about 1.57 to 1.6). Polystyrene has density of 1.05 g/$cm^3$, which is higher than density of polyethylene and polypropylene. It does not have a sharp melting point because it is amorphous (Cole, 2014). This is observed in gradual softening of the material over a wide range of temperatures. The *T*g of the polystyrene is between

ISSN No:-2456-2165

74 ºC and 105 ºC, and below its *T*g, polystyrene is hard and brittle (Biron, 2007). Reports had shown that nanocomposites are composites in which at least one of the phases shows dimensions in the nanometre range (1 nm = $10^{-9}$ m). Nanocomposite materials have emerged as suitable alternatives to overcome limitations of microcomposites and monolithics, while posing preparation challenges related to the control of elemental composition and stoichiometry in the nanocluster phase (Schmidt *et al.,* 2002). They are reported to be the materials of 21st century in the view of possessing design uniqueness and property combinations that are not found in conventional composites (Schmidt *et al.,* 2002).

It is reported that nanoparticles and nanocomposites are characterized using different techniques to get insight into their morphological structures. This involves the use of instrument such as; X-Ray Diffractometer. Characterization tools are crucial to comprehend the basic physical and chemicalproperties of metal oxides nanoparticles and polymer nanocomposites. For structural applications, it facilitates the study of emergingmaterials by giving information on some intrinsic properties (Meyyappan, 2004). Various techniquesfor characterization have been used extensively in polymer nanocomposite research (Meyyappan, 2004).This research work desires to provide information on the synthesis and characterization of $Sb_2O_3$, BaO and NiO nanoparticles via co-precipitation method. The aim of this research is to synthesize and characterize $Sb_2O_3$, BaO and NiO nanoparticles. The objective is to evaluate the crystallinity of the synthesized metal oxides nanoparticles using X-ray diffraction technique.

## II. MATERIALS AND METHODS

### *A. Materials*

The materials used include; Stop watch, magnetic stirrer JB-4A, analytical weighing balance JT 2003A.

a) Collection of Polystyrene Wastes

Polystyrene waste samples were collected from a refuse dump site located at latitude 10º17'57"N and longitude 9º50'06"E Jahun in Bauchi State Nigeria.

b) Chemicals and Reagents

In this work or research, the nanoparticles of NiO, BaO and $Sb_2O_3$ used were synthesized in the Laboratory of Department of Chemistry, Abubakar Tafawa Balewa University, Bauchi. The solvents and reagents used were obtained in the laboratory and were of great analytical reagent grade such as ethanol (Emerk Darmstadt company), toluene (BDH Laboratory reagent), methanol (Emerk Darmstadt company), sodium hydroxide (Kermel), sodium bicarbonate (Kermel Company), nickel sulphate (AR Guandong Chemicals), barium nitrate (JHD Company), antimony trichloride (Tited Biotech Ltd).

### *B. Methods*

a) Dissolution of Polystyrene (PS)

The polystyrene wastes were rinsed off and washed several times with detergent and water to remove any food or dirt particles and dried in the laboratory. The samples (PS wastes) were crushed so that they can be fit into the container. Polystyrene waste (4g) was dissolved in 20 $cm^3$ of toluene (solvent) in a conical flask and stirred for 30 minutes using magnetic stirrer of model JB-4A. The solution was then allowed to be heated for 30 minutes at 60 ºC to form a solution (Achilias *et al.,* 2009).

b) Preparation of Nanoparticles

- Preparation of BaO Nanoparticles

  In this research, a wet chemical precipitation method was used to obtain the metal oxide nanopaticles. Sodium bicarbonate (0.4 M) was added to the 0.2 M solution of barium nitrate drop wise, under constant stirring for 2 hours until addition of sodium bicarbonate solution was complete. After the completion of the reaction, the precipitates formed were allowed to settle overnight. The solution was filtered off and washed several times with distilled water until free from excess bicarbonate. A white precipitate formed was then allowed to dry in oven at 80 ºC for 1 hour and then calcined at 150 ºC for 3 hours to form the desired barium oxide nanoparticles (Prabhavathi *et al.,* 2014).

- Preparation of NiO Nanoparticles

  The method reported by Vivek *et al.* (2014) was adopted. A solution of nickel sulphate (1.0 L, 0.11 M) was taken and aqueous ammonia was added drop wise with constant stirring using magnetic stirrer of model JB-4A until the pH of 10 was reached. The precipitate formed was filtered and washed several times with distilled water. The precipitate formed was allowed to dry in oven at 70 ºC for 24 hours and calcined at 600 ºC in a muffle furnace for 5 hours to form the desired nickel oxide nanoparticles.

- Preparation of $Sb_2O_3$ Nanoparticles

  The method reported by Cheng *et al.* (2008) was used to obtain $Sb_2O_3$ nanoparticles. 0.1 M solution of antimony trichloride was dissolved in 500 $cm^3$ of ethylene glycol under vigorous stirring to form a transparent solution. Subsequently, 500 $cm^3$ of distilled water was added to the solution and stirred for 15 minutes, 6 M solution of sodium hydroxide (NaOH) was added to adjust the pH. The whole solution was stirred for 20 minutes before transferring it into an autoclave at 120 ºC. After 12 hours, the product formed was centrifuged and washed several times with distilled water and ethanol and then dried at 60 ºC for 6 hours to obtained the required antimony oxide nanoparticles ($Sb_2O_3$) (Chen *et al.*, 2008).

c) Formation of Nanocomposites

In this experiment, an *in situ* polymerization method was used to obtain the desired nanocomposites. The nanocomposites were formed by varying the concentrations of BaO, NiO and $Sb_2O_3$ nanoparticles as 0 g, 4 g and 5 g and taking the concentration of polystyrene solution as constant (30 ml). The nanoparticles were incorporated directly into the

polymer solution and stirred for 1 hour using magnetic stirrer of model JB-4A. The mixture was maintained at 60 $^0$C for 20 hours to promote in situ polymerization. The products formed were poured into excess methanol and stirred for 15 to 20 minutes and washed several times with ethanol and water. The products formed were dried in oven at 80 $^0$C overnight to obtain the desired nanocomposites.

*C. Structural Characterization*

a) X-Ray Diffraction (XRD) Study of Nanoparticles.

A Rigaku Miniflex 600 XRD with Cu K radiation (Å= 1.54 Å) at a generator voltage of 40 kV and a generator current of 50 mA was used to measure the diffraction behaviour of untreated polystyrene, nanoparticles and formulated nanocomposites. All experiments were carried out in the reflection mode at ambient temperature with 2θ varying between 2 and 70°. The scanning speed was 2.4°/ min, and the step size was 0.002°. The collected data from X-ray diffractometer were processed using Origin Pro-8 to obtain information on the structural modification of the samples. The 2θ values, inter-planar spacing (d-spacing) and full width at half maxima (FWHM) in the crystal plane were digitally determined by the machine using Bragg's equation and the crystallite size was calculated using Debye-Scherrer's equation as shown in equation 1 and 2 below (Bazeera and Irfana, 2017).

Bragg's equation $n\lambda = 2dsin\theta$ ---------- (10)

Where n=1,

θ is the half of Bragg angle

Inter-planar spacing (d-spacing) = $\frac{n\lambda}{2sin\theta}$ ----------(11)

The Debye-Scherrer's equation is shown below;

$D = \frac{K\lambda}{\beta Cos\theta}$ ----------(12)

Where K is Scherrer's constant (sharp factor) which is normally 0.9 and λ is the X-Ray wavelength, β and θ are half width of the peak and the half of Bragg angle respectively.

## III. RESULTS AND DISCUSSIONS

*A. XRD Pattern of Untreated Polystyrene*

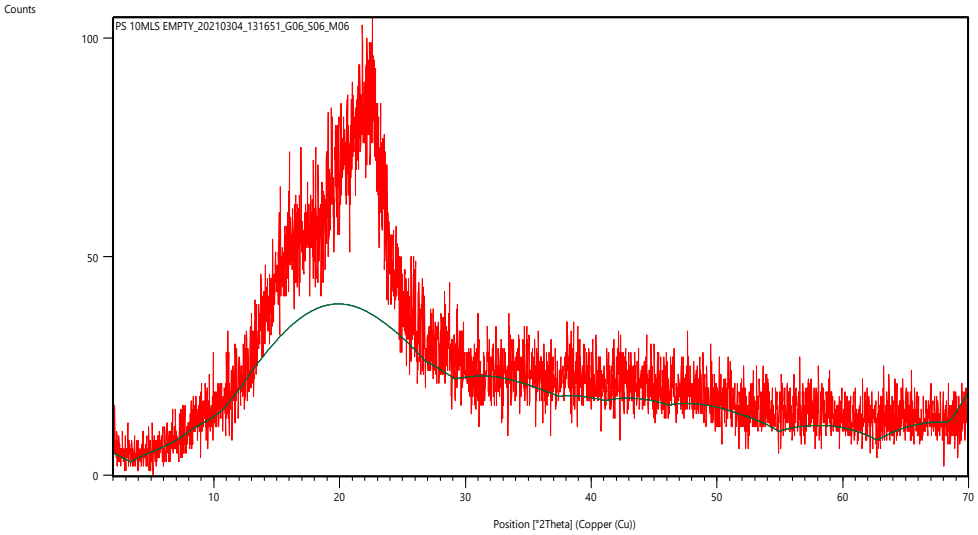


Fig. 1: XRD Pattern of Untreated Polystyrene

From Figure 1 above, can be observed that the XRD pattern specified a broad band peak for untreated polystyrene. This clearly showed that untreated polystyrene is amorphous because there is no preferred crystal orientation due to the presence of pores and the peaks are not sharp.

ISSN No:-2456-2165

*B. XRD Patterns of Synthesized Nanoparticles*

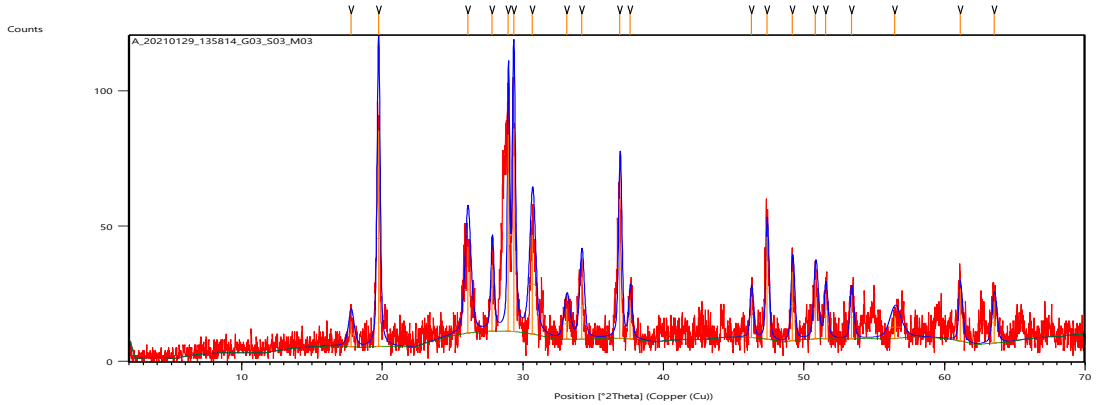


Fig. 2: XRD Pattern of $Sb_2O_3$ Nanoparticles

| Pos. (°2Th.) | Height (cts) | FWHM (°2Th.) | d-spacing (Å) | Rel. Int. (%) |
|---|---|---|---|---|
| 17.7872 | 9.28 | 0.4723 | 4.98664 | 11.62 |
| 19.7340 | 79.91 | 0.2362 | 4.49890 | 100.00 |
| 26.0836 | 31.92 | 0.4723 | 3.41633 | 39.95 |
| 27.8275 | 24.53 | 0.2362 | 3.20608 | 30.69 |
| 28.9611 | 72.73 | 0.1574 | 3.08311 | 91.02 |
| 29.3463 | 75.19 | 0.2362 | 3.04352 | 94.10 |
| 30.6794 | 36.71 | 0.4723 | 2.91424 | 45.94 |
| 33.1284 | 11.22 | 0.4723 | 2.70419 | 14.04 |
| 34.1868 | 23.15 | 0.3542 | 2.62286 | 28.97 |
| 36.9031 | 51.67 | 0.2362 | 2.43580 | 64.66 |
| 37.6358 | 14.48 | 0.2362 | 2.39005 | 18.12 |
| 46.2648 | 15.22 | 0.2362 | 1.96239 | 19.05 |
| 47.3726 | 37.84 | 0.1968 | 1.91905 | 47.35 |
| 49.1804 | 25.46 | 0.2362 | 1.85266 | 31.85 |
| 50.8244 | 21.90 | 0.3149 | 1.79652 | 27.40 |
| 51.5451 | 16.55 | 0.2362 | 1.77309 | 20.71 |
| 53.3791 | 16.20 | 0.2362 | 1.71641 | 20.27 |
| 56.4635 | 8.39 | 0.9446 | 1.62975 | 10.50 |
| 61.1091 | 19.42 | 0.2362 | 1.51652 | 24.31 |
| 63.5147 | 15.43 | 0.3149 | 1.46476 | 19.31 |

Table 1: XRD Data for Antimony oxide nanoparticles

From the result in Figure 2, the 2θ value increased with decreasing d-spacing value for $Sb_2O_3$ nanoparticles. This implies that as the 2θ value increased from 17.7872º to 63.5147º, the d-spacing value decreased from 4.98664 Å to 1.46476 Å for $Sb_2O_3$ nanoparticles, which is why we have peaks of different heights and at different positions. From Table 1 above, it can be observed that at 2θ value of 19.7340º, the relative intensity was 100 % (the most intense peak) indicating a more periodicity than other directions (that is, there is a preferred orientation of atoms in the crystals than other direction at 2θ values of 19.7340º for $Sb_2O_3$ nanoparticles. It can also be observed in Figure 2 that increase in the peak intensity led to a decrease in the full width at half-maxima (FWHM) for $Sb_2O_3$ nanoparticles which means there is high level of ordering and structural enhancement of material's crystallization (that is, where the intensity is high, the FWHM is low and vice-versa).

Using Debye-Scherrer equation, the average crystallite size (D) of $Sb_2O_3$ nanoparticle was calculated and found to be 32.3 nm. This result showed that the size of the prepared $Sb_2O_3$ nanoparticles is within the nanoscale region. This result is in agreement with the report by Davidson *et al.* (2012) in terms of sharpness of the peaks that during the characterization of $Sb_2O_3$ nanoparticles using XRD, no obvious impurities were detected in the pattern and sharp strong characteristic peaks suggested that the products formed were highly crystalline. According to the result obtained by Davidson *et al.* (2012), the size of $Sb_2O_3$ nanoparticles was determined by applying the Debye-Scherrer equation to the intensity of the peaks and was found to be 44 nm which is higher than the size of the $Sb_2O_3$ nanoparticles obtained in the present work (32.3 nm). This may be due to different reagents used in the synthesis of $Sb_2O_3$ nanoparticles.

ISSN No:-2456-2165

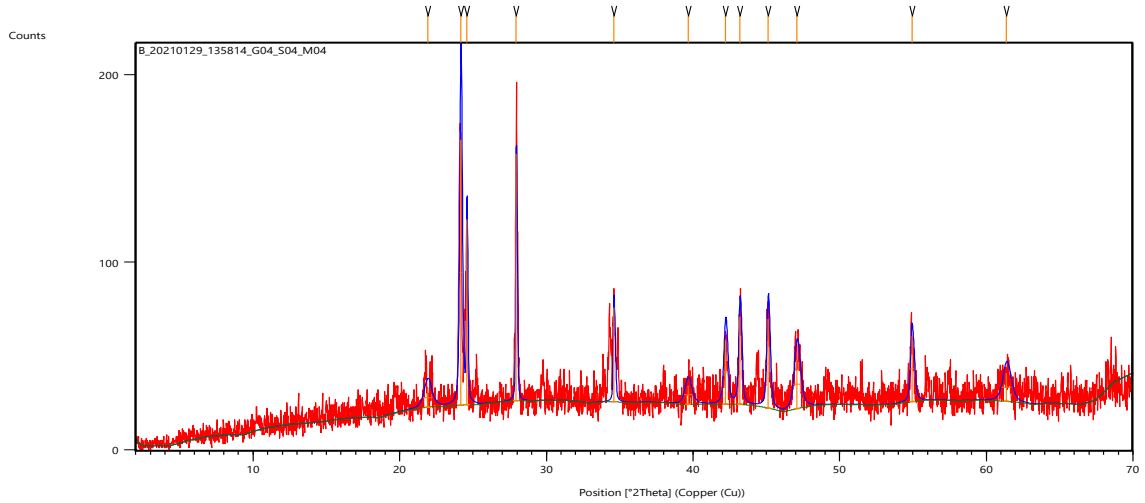


Fig. 3: XRD Patterns of BaO Nanoparticles

| Pos. (°2Th.) | Height (cts) | FWHM (°2Th.) | d-spacing (Å) | Rel. Int. (%) |
|---|---|---|---|---|
| 21.9159 | 10.39 | 0.6298 | 4.05567 | 7.35 |
| 24.1729 | 141.45 | 0.1771 | 3.68187 | 100.00 |
| 24.5847 | 98.95 | 0.0787 | 3.62113 | 69.95 |
| 27.9473 | 131.61 | 0.0787 | 3.19260 | 93.04 |
| 34.6175 | 50.39 | 0.1181 | 2.59120 | 35.62 |
| 39.6597 | 9.90 | 0.5510 | 2.27262 | 7.00 |
| 42.2122 | 34.17 | 0.2755 | 2.14092 | 24.16 |
| 43.1964 | 46.71 | 0.1968 | 2.09440 | 33.02 |
| 45.1220 | 47.58 | 0.2362 | 2.00939 | 33.64 |
| 47.0868 | 26.12 | 0.4723 | 1.93003 | 18.46 |
| 54.9275 | 34.87 | 0.2362 | 1.67163 | 24.65 |
| 61.3696 | 15.05 | 0.6298 | 1.51071 | 10.64 |

Table 2: XRD Properties of Barium Oxide Nanoparticles

From Figure 3 above, it can be observed that the characteristic peaks of BaO nanoparticles were detected indicating a purity of the synthesized BaO nanoparticles. The d-spacing value decreased with increasing 2θ value as shown in Figure 3. Sharpness of the peaks showed a well crystal growth of barium oxide nanoparticles and at 2θ value of 24.1729º, BaO nanoparticles showed relative intensity of 100 % indicating a more periodicity in the crystal.

From the result in Table 2 above, the 2θ value increased with decreasing d-spacing value for BaO nanoparticles. This implies that as the 2θ value increased from 21.9159º to 61.3696º, the d-spacing value decreased from 4.05567 Å to 1.51071 Å for BaO nanoparticles, which is why we have peaks of different heights and at different positions. From Table 2, it can also be observed that at 2θ value of 24.1729º, the relative intensity was 100 % (the most intense peak) indicating a more periodicity than other directions (that is, there is a preferred orientation of atoms in the crystals than other direction at 2θ values of 24.1729º for BaO nanoparticles. It can also be observed that increase in the peak intensity led to a decrease in the full width at half-maxima (FWHM) for BaO nanoparticles which means there is high level of ordering and structural enhancement of material's crystallization (that is, where the intensity is high, the FWHM is low and vice-versa). The average crystallite size of barium oxide nanoparticles is 46.4 nm as calculated using Debye-Scherrer equation.

This result is in agreement with the result obtained by Bazeera and Irfana (2017) that the XRD patterns for the synthesized BaO nanoparticles were recorded and the values of 2θ, d-spacing, relative intensity and Full width at half maxima (FWHM) were obtained for the XRD pattern. According to the result obtained by Bazeera and Irfana (2017), the XRD peaks obtained for BaO nanoparticles showed increase of 2θ value ranging from 19.6544º to 68.2371º and decrease of d-spacing values from 4.5131 Å to 1.3744 Å respectively. The obtained values confirmed the presence of BaO phase in the BaO nanoparticles with tetragonal crystal structures and the 'd-spacing' values for all the lines were calculated using Bragg's equation and the crystallite size was calculated using Debye- Scherrer equation and was found to be 29 nm (Bazeera and Irfana, 2017).

ISSN No:-2456-2165

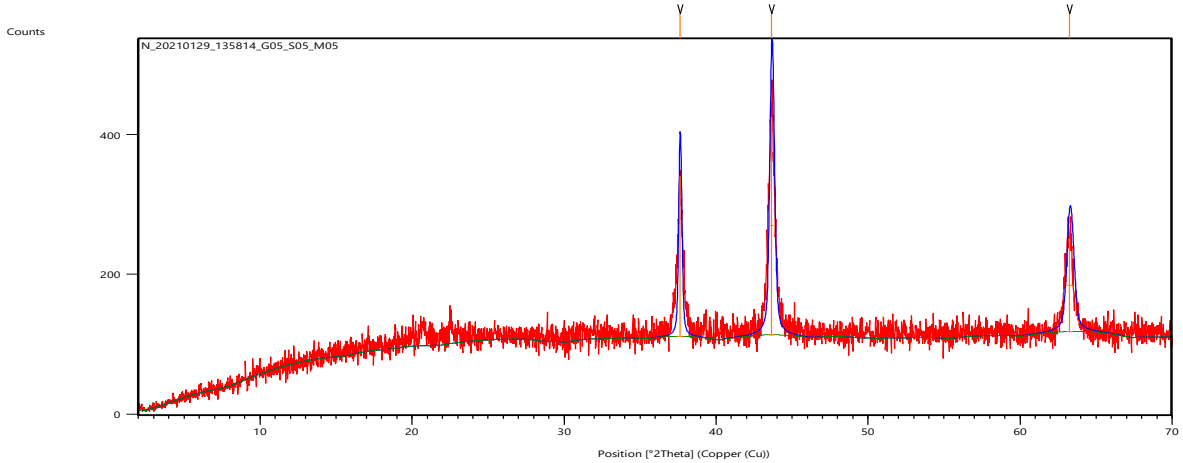


Fig. 4: XRD Patterns of NiO Nanoparticles

| Pos. (°2Th.) | Height (cts) | FWHM (°2Th.) | d-spacing (Å) | Rel. Int. (%) |
|---|---|---|---|---|
| 37.6210 | 229.13 | 0.1968 | 2.39095 | 73.53 |
| 43.6593 | 311.63 | 0.3149 | 2.07326 | 100.00 |
| 63.2621 | 132.42 | 0.4723 | 1.47000 | 42.49 |

Table 3: XRD Properties of NiO Nanoparticles

From Figure 4 above, it can also be observed that the characteristic peaks of NiO nanoparticles were detected indicating a purity of the synthesized NiO nanoparticles. The d-spacing value decreased with increasing 2θ value. Sharpness of the peaks showed a well crystal growth of NiO nanoparticles and at 2θ value of 43.6593º, NiO nanoparticles showed relative intensity of 100 % indicating a more periodicity in the crystal. From the result in Table 3, the 2θ value increased with decreasing d-spacing value for NiO nanoparticles. This implies that as the 2θ value increased from 37.6210º to 63.2621º, the d-spacing value decreased from 2.39095 Å to 1.47000 Å for NiO nanoparticles, which is why we have peaks of different heights and at different positions. It can be observed that at 2θ value of 43.6593º, the relative intensity was 100 % (the most intense peak) indicating a more periodicity than other directions (that is, there is a preferred orientation of atoms in the crystals than other direction at 2θ values of 43.6593º for NiO nanoparticles. It can also be observed in Table 3that increase in the peak intensity led to a decrease in the full width at half-maxima (FWHM) for NiO nanoparticles which means there is high level of ordering and structural enhancement of material's crystallization (that is, where the intensity is high, the FWHM is low and vice-versa). The average crystallite size of NiO nanoparticles is 31.2 nm as calculated using Debye-Scherrer equation.

This result is in agreement with the report by El-Kemary *et al.* (2013) in terms of crystallite size that the XRD patterns of the synthesized NiO nanoparticles exhibited sharpened reflection peaks which showed a growth in the crystallite size. According to the result obtained by El-Kemary *et al* (2013), the peaks positions appearing at 2θ= 37.10º, 43.30º, 62.87º, 76.50º and 79.22º which were indexed as (111), (200), (220), (311) and (222) crystal planes of the bulk NiO nanoparticles. The sharpness and intensity of the peaks indicated the well crystalline nature of the prepared NiO nanoparticles. The crystallite size based on X-ray peak broadening was estimated using Debye-Scherrer equation and was nearly 32 nm (El-Kemary *et al.*, 2013).

The overall results showed that the crystallite sizes of the synthesized $Sb_2O_3$ (32.3 nm), BaO (46.4 nm) and NiO (31.2 nm) nanoparticles are within the nanoscale region but NiO nanoparticle with the least crystallite size (31.2 nm) gave a significant properties of the material because nanoparticle larger than 50 nm size show no significant properties of the material.

*C. 3.3 Effects of Nanoparticles on the XRD Properties of Nanocomposites*

Results showing the XRD properties of nanocomposites containing antimony oxide, barium oxide and nickel oxide nanoparticles are shown below.

a) Effect of $Sb_2O_3$ Nanoparticles on the XRD Properties of $Sb_2O_3$/PS Nanocomposite

Figure 5 below showed the XRD properties of $Sb_2O_3$/PS nanocomposite containing 1 g of $Sb_2O_3$ nanoparticles. From Figure 5, it can be observed that at 2θ value of 29.1257º, the d-spacing value is 3.06352 Å, the intensity of the peak is 100 %, the height of the peak is 11.23 and the full width at half maxima (FWHM) is 1.1520 for nanocomposite containing 1 g of $Sb_2O_3$ nanoparticles.

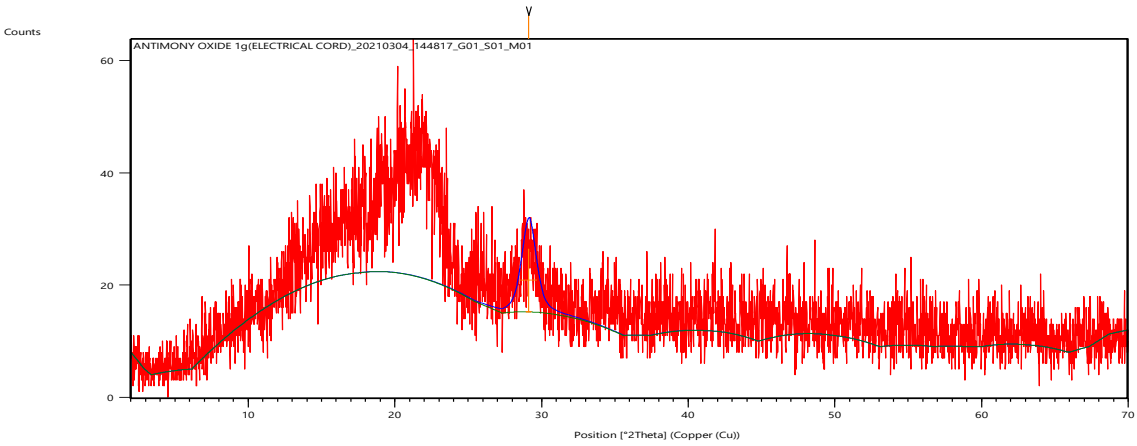


Figure 5: XRD Patterns for Nanocomposites Containing 1 g of $Sb_2O_3$ Nanoparticles

| Pos. (°2Th.) | Height (cts) | FWHM (°2Th.) | d-spacing (Å) | Rel. Int. (%) |
|---|---|---|---|---|
| 29.1257 | 11.23 | 1.1520 | 3.06352 | 100.00 |

**Table 4:** XRD Properties of 1 g of $Sb_2O_3$/PS Nanocomposites

This implies that the most intense peak is 100 % and that is the point at which the nanoparticles are more abundant and the order of arrangement of nanoparticles in the polymer has preferred orientation. This clearly showed that $Sb_2O_3$/PS nanocomposite exhibits a semi-crystalline structure due to diffraction of light at a particular single angle. The interaction between the nanoparticles and the polymer matrix and the dispersion of nanoparticles within the polymer matrix gave the nanocomposites the ability to form a conductive network and become electrically conductive, thermally conductive and better fire retarding effect due to the charge transfer complexes inside the polymer matrix.

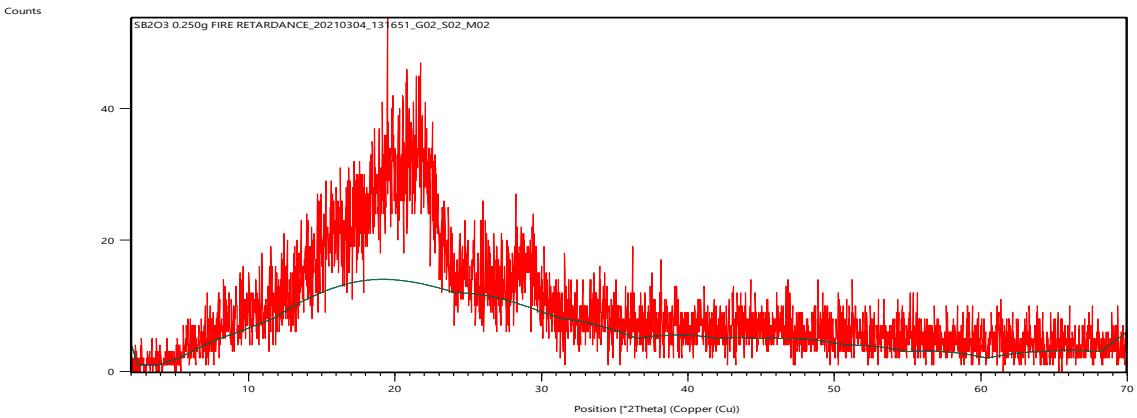


Fig. 6: XRD Pattern for Nanocomposite Containing 0.250 g of $Sb_2O_3$ Nanoparticles

The result in Figure 6 also showed the XRD properties of nanocomposites containing 0.250 g of $Sb_2O_3$ nanoparticles incorporated in the polystyrene matrix. From Figure 6, it can be observed that nanocomposite shows broad band peaks due to low concentration of nanoparticles incorporated in the polystyrene matrix which has led to a weak interaction between the nanoparticles and the polymer matrix. The result in Figure 6 also showed that the nanocomposite containing 0.250 g of $Sb_2O_3$ nanoparticles indicated an amorphous structure but gave a better fire retarding effect because Sb as a metalloid; has characteristics of both metals and non-metals.

The large surface area and crystalline nature of $Sb_2O_3$ nanoparticles as well as the homogeneous impregnation of nanoparticles within the amorphous region of the polymer (matrix) at 1 g nanoparticle content have helped in modifying the surface morphology of the polymer nanocomposite as shown in the XRD result of the $Sb_2O_3$/PS nanocomposites. This clearly showed that as concentration of nanoparticles increased, the crystallinity also increased. This has helped the polymer nanocomposites to have improved thermal, electrical, fire retarding and mechanical properties due to formation of smooth surface and conducting network.

ISSN No:-2456-2165

b) Effect of BaO Nanoparticle on the XRD Properties of BaO/PS Nanocomposite

Result showing the effect of nanoparticles on the XRD properties of formulated nanocomposites in Figure 7 and Table 5 below.

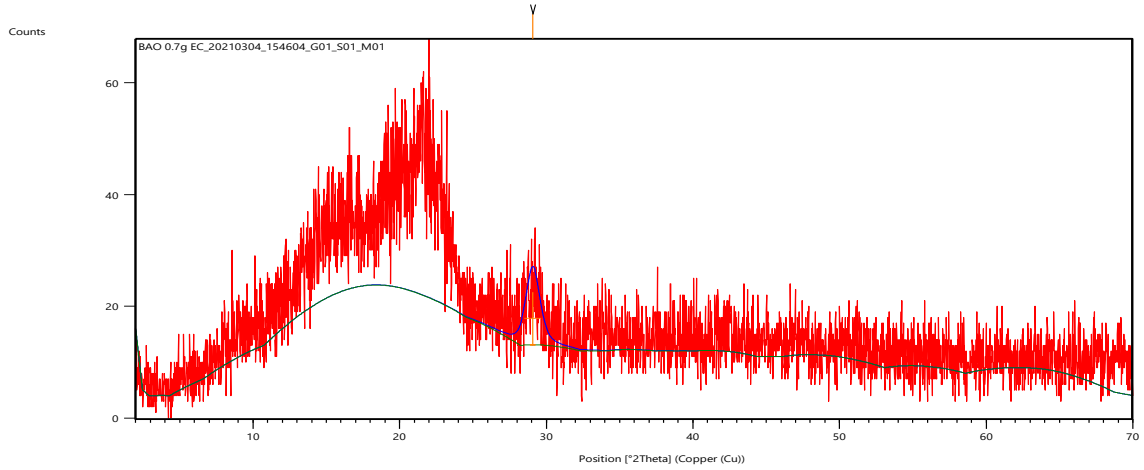


Fig. 7: XRD Patterns for Nanocomposite Containing 0.7 g of BaO Nanoparticles

| Pos. (°2Th.) | Height (cts) | FWHM (°2Th.) | d-spacing (Å) | Rel. Int. (%) |
|---|---|---|---|---|
| 29.0567 | 9.39 | 1.1520 | 3.07065 | 100.00 |

Table 5: XRD Properties of Nanocomposite Containing 0.7 g of BaO Nanoparticles

Table 5 above showed the XRD properties of BaO/PS nanocomposite containing 0.7 g of BaO nanoparticles. From the result in Table 5 and Figure 7, it can be observed that at 2θ value of 29.0567º, the intensity of the peak is 100 %, the d-spacing value is 3.07065 Å, the height of the peak is 9.39 and the full width at half maxima (FWHM) is 1.1520 for nanocomposite containing 0.7 g of BaO nanoparticles. This implies that the most intense peak is 100 % and that is the point at which the nanoparticles are more abundant and the order of arrangement of nanoparticles in the polymer has preferred orientation as shown in Figure 7 above. This clearly shows that BaO/PS nanocomposite exhibits a semi-crystalline structure due to diffraction of light at a particular single angle. The dispersion of nanoparticles within the polymer matrix and the interaction between the nanoparticles and the polymer matrix has helped to modify the nanocomposites to form a conductive network and become electrically conductive due to the charge transfer complexes inside the polymer matrix. This may be due to the fact that Ba being an alkali earth metal (light metal) has electrical and thermal conductivity property.

c) Effect of NiO Nanoparticle on the XRD Properties of NiO/PS Nanocomposite

Result showing the effect of nanoparticles on the XRD properties of formulated nanocomposites in Figure 8 and Table 6 below.

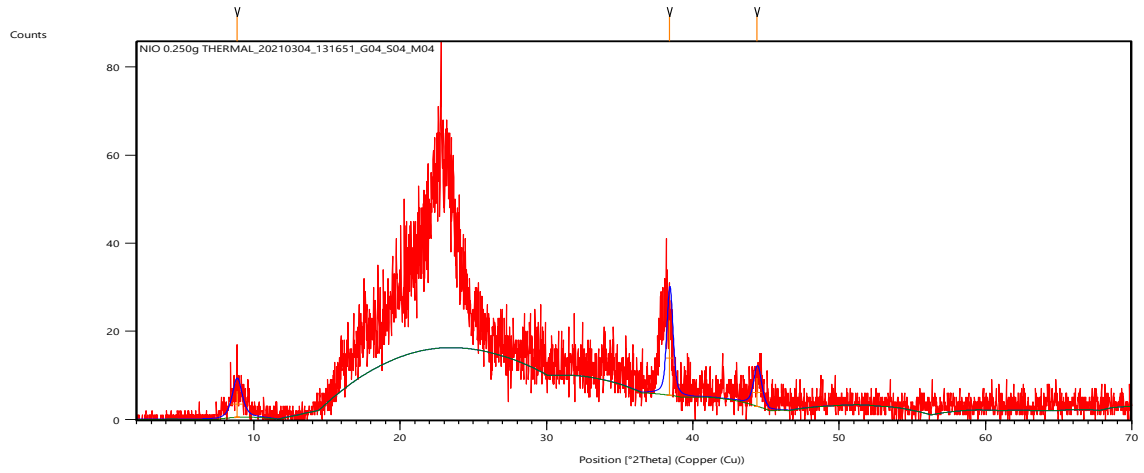


Fig. 8: XRD Patterns for Nanocomposite Containing 0.5 g of NiO Nanoparticles

ISSN No:-2456-2165

| Pos. (°2Th.) | Height (cts) | FWHM (°2Th.) | d-spacing (Å) | Rel. Int. (%) |
|---|---|---|---|---|
| 8.8637 | 6.00 | 0.7872 | 9.97678 | 35.33 |
| 38.4104 | 16.98 | 0.4723 | 2.34361 | 100.00 |
| 44.3969 | 6.36 | 0.6298 | 2.04051 | 37.43 |

Table 6: XRD Properties of Nanocomposite Containing 0.5 g of NiO Nanoparticles

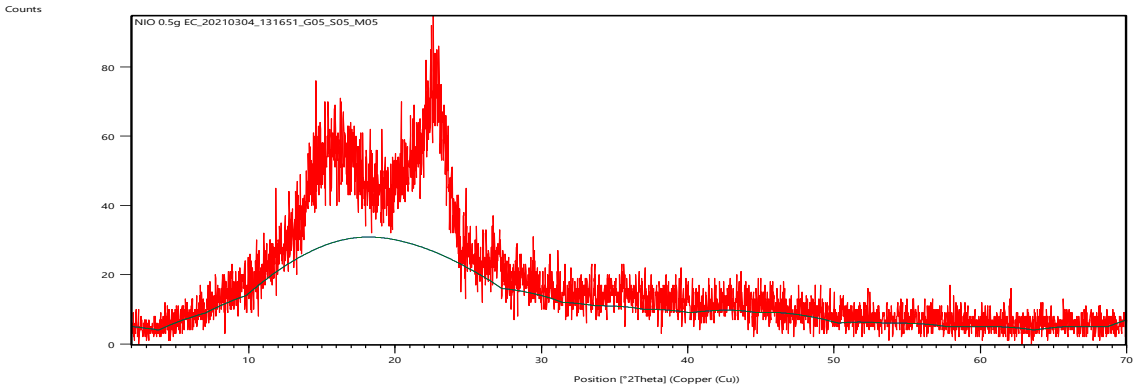


Fig. 9 : XRD Pattern for Nanocomposite Containing 0.250 g of NiO Nanoparticles

Table 6 above showed the XRD properties of NiO/PS nanocomposite containing 0.5 g of nickel oxide nanoparticles. From Figure 8 and Table 6, it can be observed that at 2θ value of 38.4104º, the intensity of the peak is 100 %, d-spacing value is 2.34361 Å, the height of the peak is 16.98 and the FWHM is 0.4723. The result in Table 6 showed that increase in the peak intensity led to a decrease in the full width at half-maxima (FWHM) for nanocomposite containing 0.5 g of NiO nanoparticles which means there is high level of ordering and structural enhancement of material's crystallization (that is, where the intensity is high, the FWHM is low and vice-versa).

Figure 9 also showed the XRD properties of nanocomposites containing 0.250 g of NiO nanoparticles incorporated in the polystyrene matrix. From Figure 9, it can be observed that nanocomposite containing 0.250 g of NiO nanoparticles shows broad band peaks due to low concentration of NiO nanoparticles incorporated in the polystyrene matrix which has led to a weak interaction between the nanoparticles and the polymer matrix. The XRD properties in Figure 9 showed that the nanocomposite containing 0.250 g of NiO nanoparticles indicated an amorphous structure.

The result in Table 6 clearly showed that NiO/PS nanocomposite exhibits a semi-crystalline structure due to diffraction of light at a particular single angle. The dispersion of nanoparticles within the polymer matrix and the interaction between the nanoparticles and the polymer matrix has helped to modify the nanocomposites to form a conductive network and become electrically conductive due to the charge transfer complexes inside the polymer matrix. This may be due to the fact that Ni being a transition metal (heavy metal) has high electrical and thermal conductivity property.

## IV. CONCLUSION

Based on the present findings, it can be concluded that Sb2O3, NiO and BaO nanoparticles were synthesized via chemical precipitation method and PS/NiO, PS/BaO and PS/Sb2O3 nanocomposites were produced. The crystallinity of the nanoparticles and formulated nanocomposite were evaluated and the modifications of the untreated polystyrene and formulated nanocomposites were characterized using XRD technique.

## V. ACKNOWLEDGEMENT

The authors wish to thank Alhaji Sabo Takko family for their support financially and morally. The authors are also grateful to the Department of Chemistry, Abubakar Tafawa Balewa University, Bauchi Nigeria for the successful conduct of the research.

## REFERENCES

[1.] Achilias D.S., Antonakou W., Koustsokosta E., and Lappas A. (2009) Chemical Recycling of Polymers from WEEE. *Journal of Applied Polymer Science.* 114:6, 212-221

[2.] Ashik U.P.M., Shinji K., and Hayashi. J. (2018). Synthesis of inorganic nanomaterials. Fukuoka Japan. Pp 19-57

[3.] Batista, C. A., Silvera, L., Ronald, G., and Kotov, N. A. (2015). "Nonadditivity of nanoparticle interactions". *Science.*350 (6257): 1242477.

[4.] Bazeera Z. A., and Irfana A. M (2017). Synthesis and Characterization of Barium Oxide Nanoparticles. *Journal of Applied Physics (IQSR-JAP)*. Pp 76-80

[5.] Biron, M. (2007). *Thermoplastics and thermoplastic composites*; Butterworth-Heinemann, Elsevier: Oxford, UK.

[6.] Chen, X.Y., Huh, H. S., and Lee, S. W. (2008). Synthesis of antimony oxide by hydrothermal method. *Journal of solid state chemistry*. 181: 2127
[7.] Cole, L. [Ed.] (2014). Polystyrene Synthesis, Characterization and Application. New York; Nova Publishers, Inc. Pp 1-2, 205-206, 201-212, 213-230.
[8.] Davidson S., Kaviyarasu K., and Prem A. (2012). A Rapid and Versatile Method for Solvothermal Antimony Oxide Nanocrystals Under Mild Conditions. *Applied Nanoscience*. 12: 1-6
[9.] El-Kemary M; Nagy N; and El-Mehasseb (2013). Nickel Oxide Nanoparticles; Synthesis and Spectral Studies of Interaction with Glucose. *Material Science in Semiconductor Processing.* 16: 1747-1752.
[10.] Heinzerling P., and Oetken M. (2018). Nanochemistry-A split between 18th Century and Modern Times. *World Journal of Chemical Education.*6(1):1-7
[11.] Meyyappan, M. (ed.). (2004). Carbon Nanotubes, Science and Application, CRC. (Reproduced in part with permission from Taylor and Francis, USA _ 2006.).
[12.] Prabhavathi P. S. J., Punitta, P., Shameela R. R., Ranjith, G., Suresh, N. M., D.Manithamithu. . (2014). Method of synthesis of copper oxide, zinc oxide, lead oxide and barium oxide nanoparticles. *Journal of Chemical and Pharmaceutical Research*, 6(3):1472-1478.
[13.] Schmidt, D, Shah, D., Giannelis, E. P. (2002). New advances in polymer/layered silicate nanocomposites. *Current Opinion in Solid State & Materials Science*. 6(3):205-212.
[14.] Vivek, S. J., Avnish, K. A., Mayank, K., Vishnu Dev., Joginder Singh (2014) Synthesis and Characterization of Chromium Oxide Nanoparticles. *Oriental Journal of Chemistry*.30:2 Pp 559-566.
[15.] Yuehua, H., Huihui, Z., and Huaming, Y. (2007). Direct Synthesis of $Sb_2O_3$ Nanoparticles via Hydrolysis-Precipitation Method. *Journal of Alloys and Compounds*. 428:327-331.